USAARL Report No. 2001-06

Final Phase One Evaluation of the Microvision, Inc. Aircrew Integrated Helmet System (AIHS) HGU-56P Scanning Laser Display

by
Thomas H. Harding, John S. Martin, and Howard H. Beasley (UES, Inc.) and
Clarence E. Rash (USAARL)

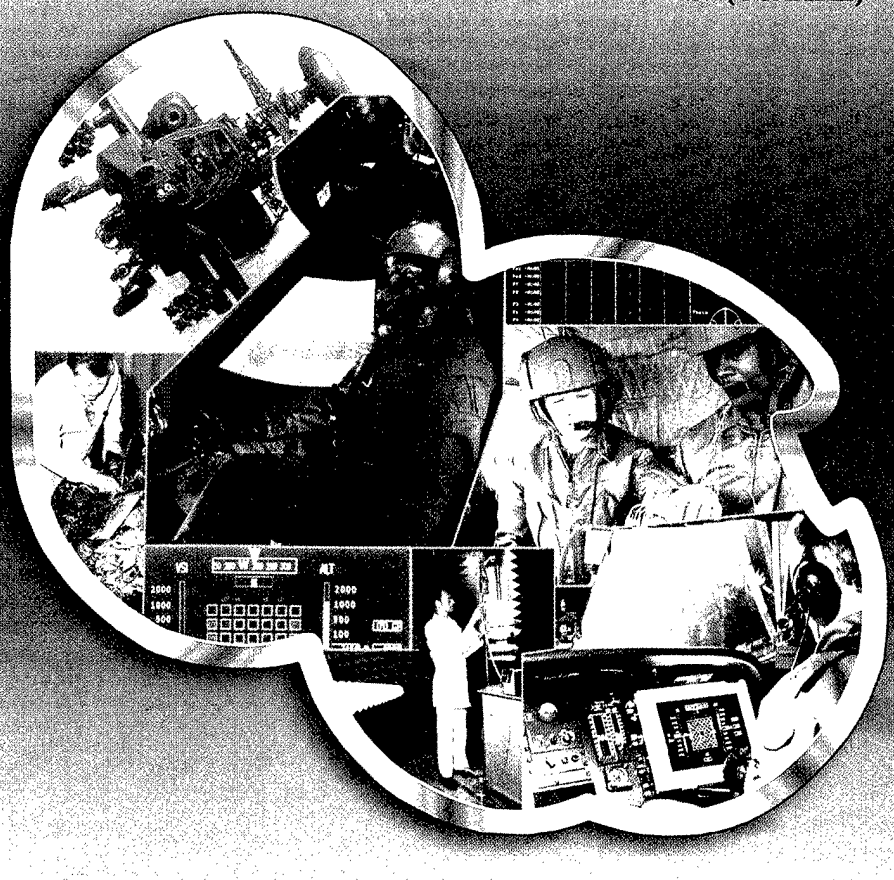

Aircrew Health and Performance Division

June 2001

USAARL

U.S. Army
Aeromedical Research
Laboratory

Notice

Qualified requesters

Qualified requesters may obtain copies from the Defense Technical Information Center (DTIC), Cameron Station, Alexandria, Virginia 22314. Orders will be expedited if placed through the librarian or other person designated to request documents from DTIC.

Change of address

Organizations receiving reports from the U.S. Army Aeromedical Research Laboratory on automatic mailing lists should confirm correct address when corresponding about Laboratory reports.

Disposition

Destroy this document when it is no longer needed. Do not return it to the originator.

Disclaimer

The views, opinions, and/or findings contained in this report are those of the author(s) and should not be construed as an official Department of the Army position, policy, or decision, unless so designated by other official documentation. Citation of trade names in this report does not constitute an official Department of the Army endorsement or approval of the use of such commercial items.

REPORT DOCUMENTATION PAGE

Form Approved
OMB No. 0704-0188

1a. REPORT SECURITY CLASSIFICATION
Unclassified

1b. RESTRICTIVE MARKINGS

2a. SECURITY CLASSIFICATION AUTHORITY

3. DISTRIBUTION / AVAILABILITY OF REPORT
Approved for public release, distribution unlimited

2b. DECLASSIFICATION / DOWNGRADING SCHEDULE

4. PERFORMING ORGANIZATION REPORT NUMBER(S)
USAARL Report No. 2001-06

5. MONITORING ORGANIZATION REPORT NUMBER(S)

6a. NAME OF PERFORMING ORGANIZATION
U.S. Army Aeromedical Research Laboratory

6b. OFFICE SYMBOL (If applicable)
MCMR-UAD

7a. NAME OF MONITORING ORGANIZATION
U.S. Army Medical Research and Materiel Command

6c. ADDRESS (City, State, and ZIP Code)
P.O. Box 620577
Fort Rucker, AL 36362-0577

7b. ADDRESS (City, State, and ZIP Code)
Fort Detrick
Frederick, MD 21702-5012

8a. NAME OF FUNDING / SPONSORING ORGANIZATION

8b. OFFICE SYMBOL (If applicable)

9. PROCUREMENT INSTRUMENT IDENTIFICATION NUMBER

8c. ADDRESS (City, State, and ZIP Code)

10. SOURCE OF FUNDING NUMBERS

PROGRAM ELEMENT NO.	PROJECT NO.	TASK NO.	WORK UNIT ACCESSION NO.
62787A	30162787A879	PB	DA336445

11. TITLE (Include Security Classification)
Final Phase One Evaluation of the Microvision, Inc. Aircrew Integrated Helmet System (AIHS) HGU-56P Scanning Laser Display

12. PERSONAL AUTHOR(S)
Thomas H. Harding, John S. Martin, Howard H. Beasley, Clarence E. Rash

13a. TYPE OF REPORT	13b. TIME COVERED FROM	TO	14. DATE OF REPORT (Year, Month, Day)	15. PAGE COUNT
Final			2001 June	30

16. SUPPLEMENTAL NOTATION

17. COSATI CODES		
FIELD	GROUP	SUB-GROUP

18. SUBJECT TERMS (Continue on reverse if necessary and identify by block number)
Helmet Mounted Display (HMD), Virtual Retinal Display (VRD), Aircrew Integrated Helmet System (AIHS), Optical Testing, Helmet Gear Unit-56P (HGU-56P)

19. ABSTRACT (Continue on reverse if necessary and identify by block number)

In support of the RAH-66 Comanche, Microvision, Inc., Seattle, Washington, has developed a prototype helmet mounted display (HMD) based on laser sources. This report is the second evaluation of the Microvision system. This system has been tested for both optical and visual performance. Tests include exit pupil size (shape and uniformity), field-of-view, luminance, contrast, contrast transfer function (CTF), modulation transfer function (MTF), color discrimination, and optical focus.

20. DISTRIBUTION / AVAILABILITY OF ABSTRACT
☒ UNCLASSIFIED/UNLIMITED ☐ SAME AS RPT. ☐ DTIC USERS

21. ABSTRACT SECURITY CLASSIFICATION
Unclassified

22a. NAME OF RESPONSIBLE INDIVIDUAL
Chief, Science Support Center

22b. TELEPHONE (Include Area Code)
(334) 255-6907

22c. OFFICE SYMBOL
MCMR-UAX-SI

DD Form 1473, JUN 86 *Previous editions are obsolete.*

Table of contents

Page

Introduction 1

System tests 3
- Exit pupil size and shape 4
- Eye relief 6
- Field-of-view (FOV) and binocular overlap 7
- Binocular alignment 9
- Transmissivity 10
- Spectral output 11
- Aberrations 12
- Luminance response (Gamma) 13
- Luminance uniformity 14
- Contrast 16
- Contrast transfer function (CTF) 17
- Modulation transfer function (MTF) 19
- Interpupilary distance (IPD) and vertical adjustments 20
- See-through color discrimination 21

Problematic features associated with jitter 22

Safety issue 22

Summary and discussion 23

Reference 25

Appendix - List of manufacturers 26

List of figures

1. Microvision HMD 2

2. Electronic enclosure for the lasers, video interface and associated electronics 2

3. HMD on rotating stage showing camera image of exit pupil 3

4. Exit pupil images 4

5. Luminance profiles from the horizontal meridian of the left side exit pupil 5

Table of contents (continued)
List of figures (continued)

Page

6. Depiction of optical eye relief (distance A to C) and physical eye relief (distance B to C) 6

7. Binocular FOV schematic 8

8. Transmittance of the left channel 10

9. Spectral output of the laser based Microvision HMD 11

10. Field curvature and astigmatic error as a function of decentration 12

11. Luminance response curves as a function of applied voltage (expressed in volts) 13

12. Luminance uniformity of a 25-square pattern dispersed evenly over the entire left side FOV. 15

13. Typical CTFs for the left (A) and right (B) sides 18

14. Left side MTFs 19

List of tables

1. Physical and optical eye relief (in mm) 6

2. FOV measurements 7

3. Luminance uniformity (deviation from the mean) 14

4. a) Lateral contrast ratios and b) Vertical contrast ratios 16

5. Evaluation summary 24

Introduction

The project manager, Aircrew Integrated System (PM-ACIS), Huntsville, Alabama, established a program with Microvision, Inc., Seattle, Washington, to develop a technology demonstrator to determine the capability of a scanning laser display to meet RAH-66 Comanche helmet mounted display (HMD) performance specifications. Under this program, titled Aircrew Integrated Helmet System (AIHS) HGU-56P VRD (Virtual Retinal Display) system, Microvision developed and delivered to the Army a laser based HMD for evaluation by the U.S. Army Aeromedical Research Laboratory (USAARL), Fort Rucker, Alabama. USAARL Report No. 99-18 was an evaluation of an earlier "concept" version of the Microvision HMD. This report constitutes the findings of an evaluation of the HMD that is a modified version of one evaluated earlier. Essentially, Microvision, Inc. made changes to the system to increase the higher spatial frequency response of the system. Indeed, minor improvements were noted in the modulation transfer function (MTF), especially in the vertical spatial frequencies. It is anticipated by Microvision engineers that a future redesign of the HMD's electronics will improve the horizontal MTF as well.

The Microvision HMD system (Figure 1) consists of several primary components: an HMD comprised of a Pilot Retained Unit (PRU) (helmet) and an Aircraft Retained Unit (ARU); an electronic and control module (Figure 2); interconnect cables and three lap top computers, two of which control imagery to the two sides of the HMD, and the third which provides control of the electronic components; as well as a power supply which provides an external voltage source for controlling the luminance of the HMD imagery. The HMD is a binocular optical system custom fitted to a Gentex HGU-56P aviation helmet. The cabinet houses the lasers, associated electronics, acousto-optical modulators, and power supplies. Fiber optic bundles bring the laser based images to the HMD's optical assemblies that contain high speed microscanners which provide a rastered image via relay optics to the eye. The Microvision HMD relay optics include two oculars which are based on a catadiopic design. The oculars consist of dual beamsplitters.

In order to achieve sufficient image resolution (1280 by 960) within the desired frame period, four laser beams were used in parallel to create the image. The lasers were aligned by Microvision engineers in order to maintain appropriate spacing between the lines. A misalignment of these lasers may be reflected in the vertical MTF of the system.

The video was a standard computer format of 1280 by 1024 pixels with 8 bits per color at 60 Hz refresh. The HMD displayed only 1280 by 960 of the 1280 by 1024 video image. Only the green 8 bit signal was used to drive the monochrome display. The output from the laptops was further controlled by a main computer that controlled the imagery reaching the HMD.

Figure 1. Microvision HMD

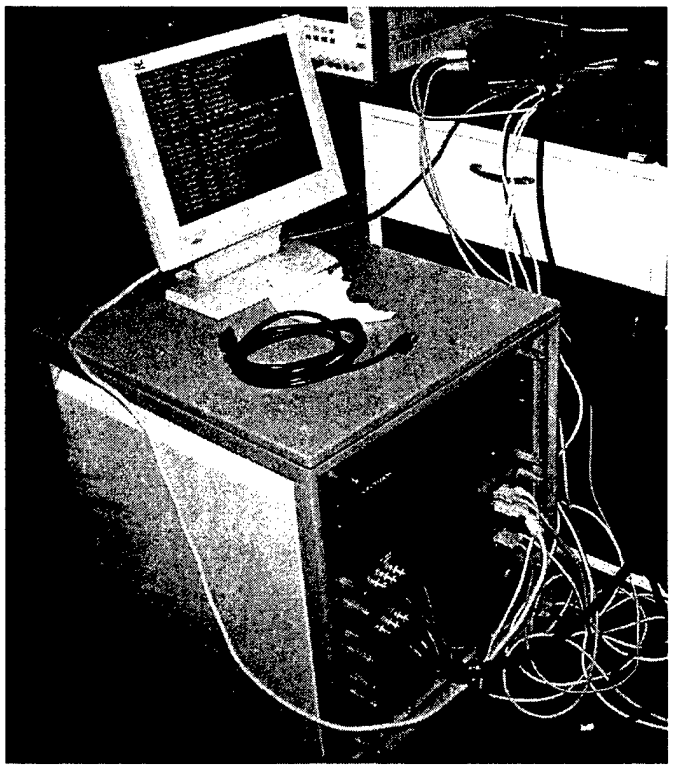

Figure 2. Electronic enclosure for the lasers, video interface and associated electronics.

System tests

In the past, many of our tests were conducted with the HMD mounted on a rotating stage with the exit pupil of the channel being measured centered directly over the center of rotation of the stage (Figure 3). As the stage was rotated in either direction, adjacent imagery came into view as if seen from a single point in space. In this way, any point along the horizontal axis could be viewed and photometrically measured. However, with the present HMD, we found that during the act of rotating the HMD the imagery was modified due to mechanical tension from the fiber optic cables. Also, the tension on the cables produced errors in rotation such that exact angular measurement could not be made. So to correct this problem, many of our measurements in this evaluation were performed by photographic analysis of imagery. A calibrated video camera with a 5 mm aperture was placed at the exit pupil so that the exit pupil was well centered on the aperture and the HMD imagery was well focused. To be sure of alignment and the ability to replicate alignment, we used a laser alignment procedure that provided consistently reliable results. The video imagery was captured by a computer image capture card and the imagery was stored for later analysis. Much of the analysis was performed using Matrox Image Inspector Software, Version 3.

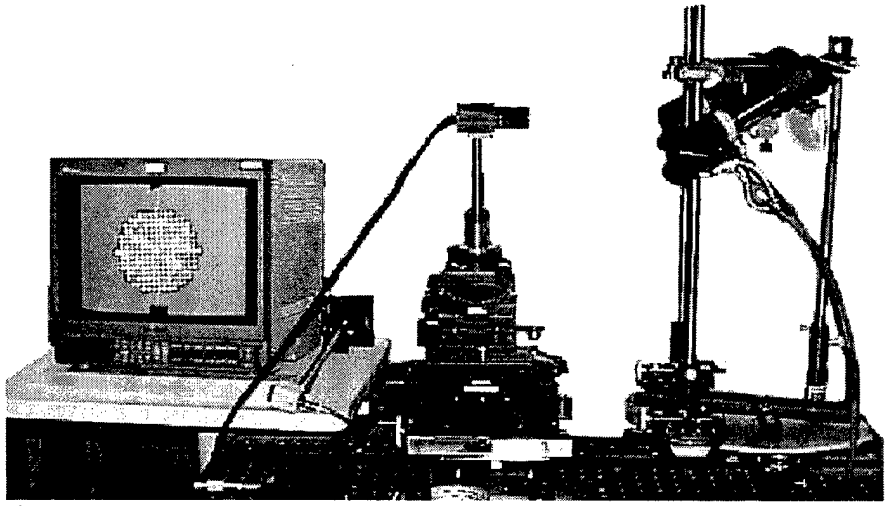

Figure 3. HMD on rotating stage showing camera image of exit pupil.

Exit pupil size and shape

Test equipment: Charge-coupled detector (CCD) video camera, monitor, computer, image capture card, millimeter rule, and Matrox Image Inspector Software, Version 3.

Test procedure: A grid pattern was displayed on the HMD with the center pixel clearly indicated. The camera was focused to infinity and was aligned with the center pixel of the left or right display. Proper alignment required the center pixel to be in the middle of the monitor with best focus over the entire monitor image. Once proper alignment was achieved, the camera was refocused on the exit pupil (Figure 4), and the HMD alignment image was replaced with a uniform field of high luminance. This image filled the exit pupil with light, and the image of the exit pupil was digitized and stored on a computer for later analysis. With camera focus fixed at the exit pupil, a millimeter rule was imaged on the monitor with the same focal distance and then digitized. This image of the rule provided the basis for calibrated measurements. The luminance uniformity of the exit pupil was assessed by evaluating the image intensity in the captured image.

Results: Figure 4 shows the exit pupil captured from the left side compared to the exit pupil captured from the same side during the previous testing (Rash et al., 1999). The current exit pupil is more uniform than the previous sample. The center beamlett still has greater luminance and this is a consequence of the diffraction technology. Figure 5 shows the luminance profile of the horizontal meridian of the exit pupil showing better uniformity in the current sample. Comanche requirements specify an exit pupil of 15 mm, and the new exit pupil appears to meet this requirement.

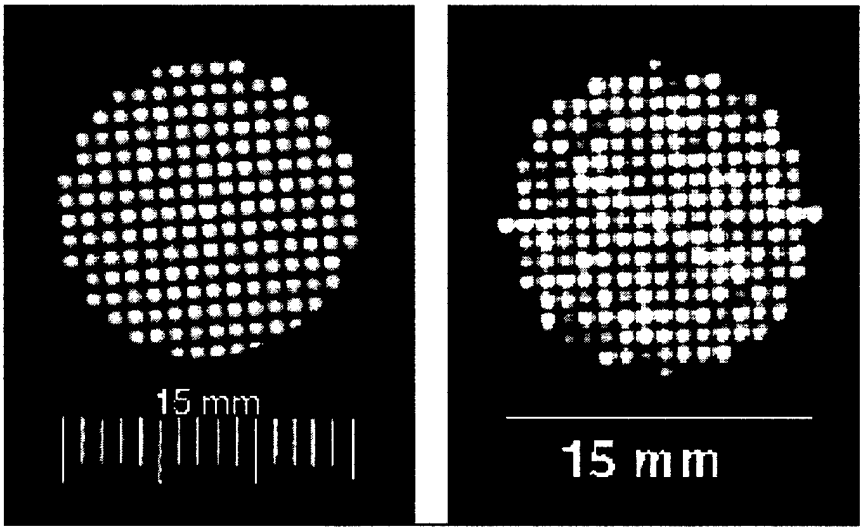

Figure 4. Exit pupil images. The image of the exit pupil on the left is the current left side exit pupil. Microvision engineers made significant progress in developing an exit pupil with rather uniform luminance. For comparison, the image on the right was captured during the earlier evaluation. (Rash et al., 1999)

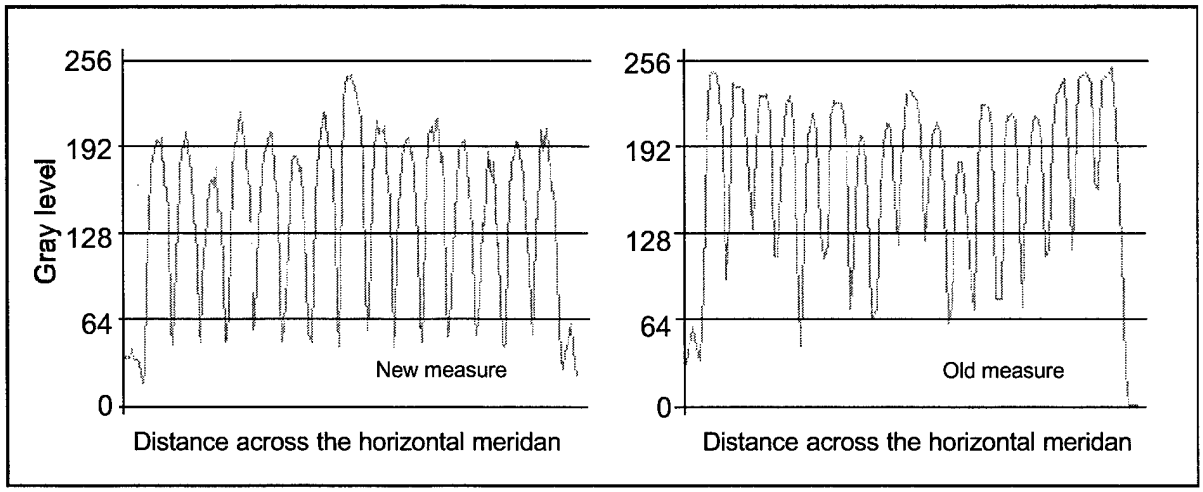

Figure 5. Luminance profiles from the horizontal meridian of the left side exit pupil. The new measure refers to the most recently measured exit pupil and the old measure refers to the exit pupil measured previously (Rash, et al., 1999). The data presented here were measured on the photographs shown in Figure 4. Note the uniformity of the luminance troughs in the new measure compared to the old.

Discussion: The horizontal and vertical exit pupil diameter is close to the specified 15 mm. As can be seen in Figure 4, the exit pupil shape is circular in nature and shows greater uniformity than the previous configuration.

Eye relief

Test equipment: Rear projection screen, video camera and monitor, and precision positioners.

Test procedure: A rear projection screen was used to locate the exit pupil position. This was accomplished by moving the rear projection screen along the optical axis until best focus was achieved (Figure 6). Eye relief can be expressed as physical eye relief or optical eye relief. Physical eye relief (eye clearance distance) is defined, for the purpose of this report, to be the straight line distance from the cornea (positioned at the exit pupil) to the vertical plane defined by the first encountered physical structure of the system. Optical eye relief is the straight line distance from the cornea to the last optical element of the HMD system. In most cases, physical eye relief is much less than optical eye relief and is more relevant in addressing compatibility with life support equipment (i.e., gas mask, oxygen mask, spectacles, etc.). Once the rear projection screen was placed at the exit pupil, a camera mounted on precision positioners was placed to the side in order to observe the distance relationship between the exit pupil and the rear lens in the catadioptic design. By moving the camera laterally, we were able to measure the distance between the rear projection screen and the center and rear edge of the catadiopic design.

Results: Table 1 presents the physical and optical eye relief values. Please note that the physical eye relief is less than the 25 mm required to accommodate a protective mask. New measurements for the right side were not taken. Those measurements shown for the right side were taken previously (Rash et al., 1999).

Table 1.
Physical and optical eye relief (in mm).

	Left side	Right side
Physical eye relief	18.9	19.0
Optical eye relief	44.0	40.5

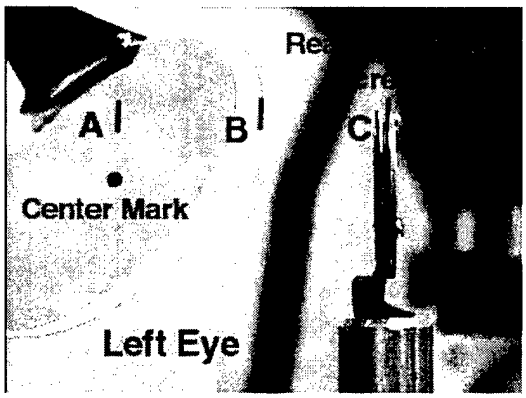

Figure 6. Depiction of optical eye relief (distance A to C) and physical eye relief (distance B to C). The rear screen projection material is collocated at the exit pupil position.

Discussion: At a measured value of 19 mm, the physical eye relief is insufficient for use with a chemical protective mask.

Field-of-view (FOV) and binocular overlap

Test equipment: CCD camera with wide angle lens, monitor, laser pointer and positioner, and a tangent screen.

Test procedure: Binocular FOV was measured by imaging a 1280 by 960 pixel pattern that clearly marked the outer borders of the image. This image was viewed by a camera that was aligned with the center of each channel's optical path, and a 5 mm aperture affixed to the camera lens was well positioned at the exit pupil. To determine FOV, the camera was set to infinity focus, and the image was viewed on a monitor. A laser pointer mounted to a positioner was aimed at points on a front tangent screen which coincided with the borders of the FOV. Each point so mapped was marked with a pin. Also, the centers of the left and right FOV were mapped in like fashion. Once all points were mapped, distance measurements were made which allowed calculation of FOV measures based upon trigonometric equations.

Results: The resultant data from the distance measurements are shown in Table 2 and in Figure 7. All data are presented in degrees. The binocular FOV was 53.24 degrees with an overlap of 25 degrees.

Table 2.
FOV measurements.

Lateral FOV	53.24
Left Horiz. FOV	41.03
Left Vert. FOV	32.36
Right Horiz. FOV	41.46
Right Vert. FOV	30.84
Center Separation	13.22
Horizontal Overlap	25
Left Side Monocular	13.76
Right Side Monocular	14.48

Discussion: The Comanche requirement of monocular FOV of 30 by 40 degrees is met.

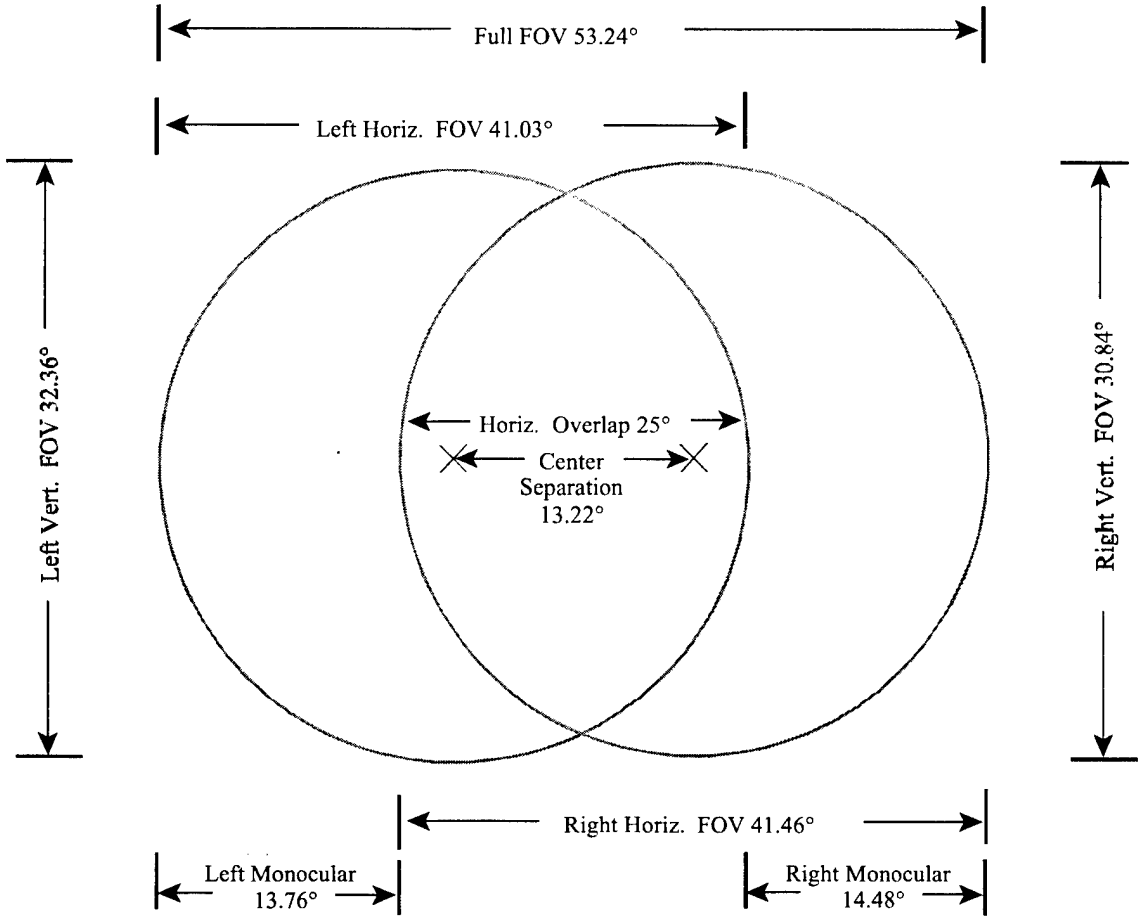

Figure 7. Binocular FOV schematic.

Binocular alignment

Test equipment: Laser, collimated night vision goggle (NVG) test device from the NVG Test Set (TS-3895A/UV), and a tangent screen.

Test procedure: For this test, each ocular was set at its mid-point. A laser projected into one side of the collimated NVG test device produced a second laser beam parallel to the first with the distance separating the two beams equal to the interpupillary distance (IPD). Having two parallel laser beams allowed testing of the see-through alignment of the HMD optics. The two laser beams were projected onto a tangent screen and their positions marked. Without moving the laser or collimated test device, we placed the HMD into the optical path such that the beams passed through the HMD's optics. Following proper alignment, the position of the laser beams were plotted on the tangent screen and the HMD's deviation from normal was calculated.

Results: The position of the laser beams with and without the optics in place were within ± 1 milliradian.

Discussion: The binocular alignment was within Comanche specification.

Transmissivity

Test equipment: A RS-12 standard tungsten lamp, a Photo Research PR704 Spectrascan™, and a computer.

Test procedure: The RS-12 standard lamp was placed in front of the left optical lens assembly with the lamp surface orthogonal to the optical axis. With the lens assembly retracted, down position, a spectral scan of the lamp was made and stored on computer. The lens assembly was then placed in position to intersect the lamp, and the spectral scan was repeated. The second scan was then divided by the first scan to find the attenuation in light due to the HMD optics. These data were then plotted as a transmissivity curve. This procedure was then repeated for the right channel.

Results: The results are shown in Figure 8.

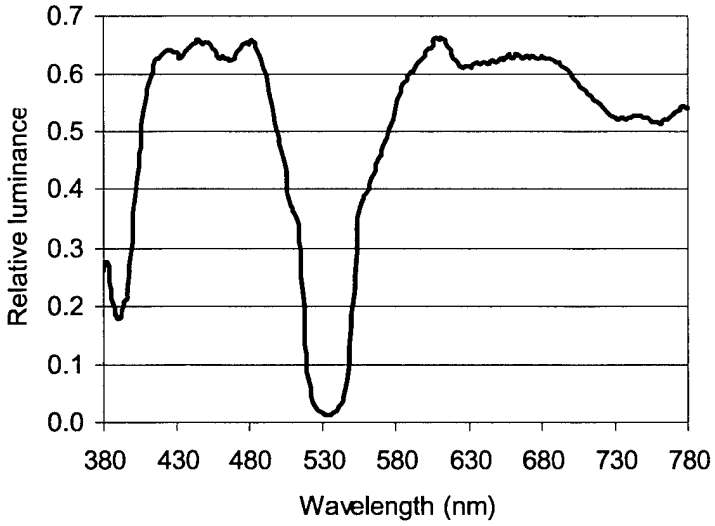

Figure 8. Transmittance of the left channel. The large notch near the peak wavelength of the laser is intended to increase reflectance of these wavelengths in order to increase the source luminance reaching the eye. The photopic transmittance (with a tungsten source) is 59.3 percent. Transmittance through the right channel was essentially identical.

Discussion: Given the high luminance nature of the HMD, the notch bandwidth of 42 nm seems large given the near monochromatic nature of the source. The large notch results in decreased see-through luminance and leads to a degradation in color discrimination and loss of contrast.

Spectral output

Test Equipment: Photo Research PR704 Spectrascan.™

Test Procedure: The spectral distribution of the light output from the HMD was measured using a Photo Research PR704 Spectrascan.™ The PR704 provided a fast scan, and the scan was highly repeatable. The bandwidth measured was only 4 to 5 nm (please note that the Spectrascan measures in 2 nm increments so a precise description cannot be made).

Results: The spectral distribution of the light reaching the eye can be seen in Figure 9.

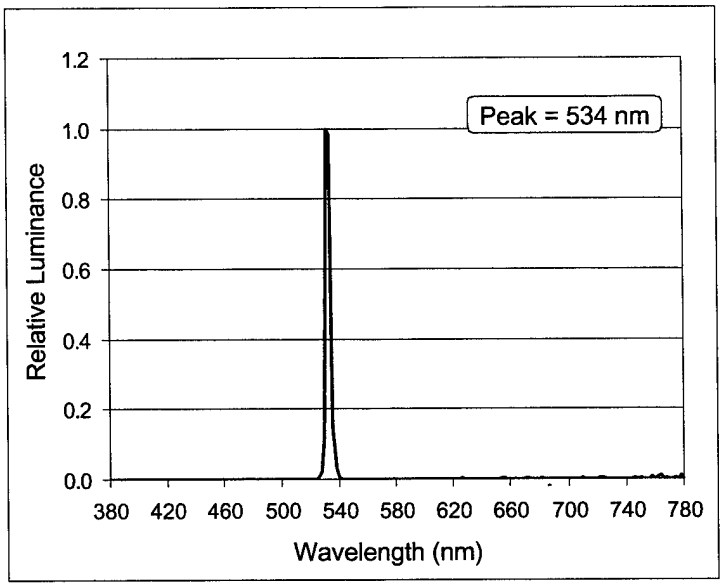

Figure 9. Spectral output of the laser based Microvision HMD.

Discussion: The high monochromaticity is characteristic of laser sources.

Aberrations

Test Equipment: Rotating and translation stages and a calibrated dioptometer.

Test Procedure: An image of a grid pattern with vertical and horizontal lines was presented to the left side of the HMD. The dioptometer with a 5 mm artificial pupil was placed at the exit pupil. An observer viewed the grid pattern with the dioptometer and focused on the vertical lines and then focused on the horizontal lines. Measurements of the dioptometer's readings were made for each focus adjustment. Field curvature, spherical and astigmatic aberrations were measured. Field curvature was measured by rotating the HMD about a central axis and taking measurements every 1 degree over the extent of the FOV. Spherical aberration was measured by holding the HMD fixed and translating the dioptometer to either side of the central axis. Measurements could be made to about 6 mm to either side of the central axis due to the size of the exit pupil. The difference between the vertical and horizontal adjustment provided an estimate of spherical aberration or astigmatic error.

Results: Aberrations were generally negative but did not exceed a -1 diopter. Astigmatic error was less than 0.5 diopter. See Figure 10.

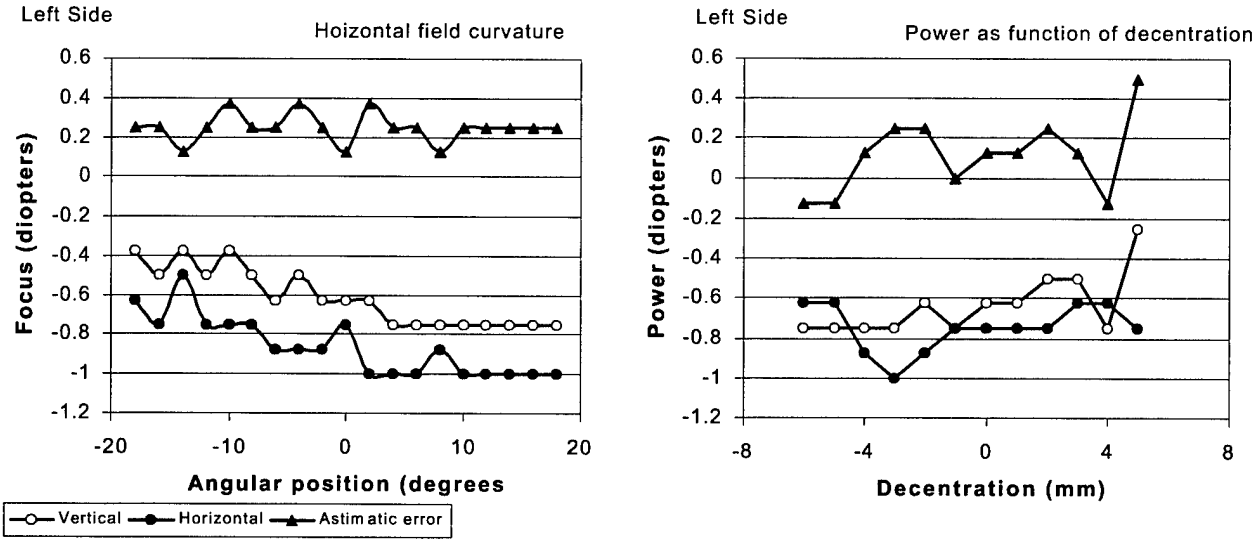

Figure 10. Field curvature and astigmatic error as a function of decentration. Data collected on left side.

Discussion: The optics appeared good and had only minimal optical aberrations.

Luminance response (Gamma)

Test equipment: Model 1980A Prichard photometer with a 5-mm iris.

Test procedure: To measure the Gamma, a 40 pixel square target in the middle of the display was turned on and set to a gray level of 0 to 255, in increments of 5. The applied voltage was set to 1.0 volt. The photometer was focused to infinity and aligned with the middle of the square. A reading was made for each of the gray level settings. This procedure was repeated for four additional fractional voltage levels to see if applied voltage affected the luminance response characteristic.

Results: Results are shown in Figure 11. The five curves are essentially the same with only a gain change. The compressive curves were monotonic with a saturation characteristic at high gray levels.

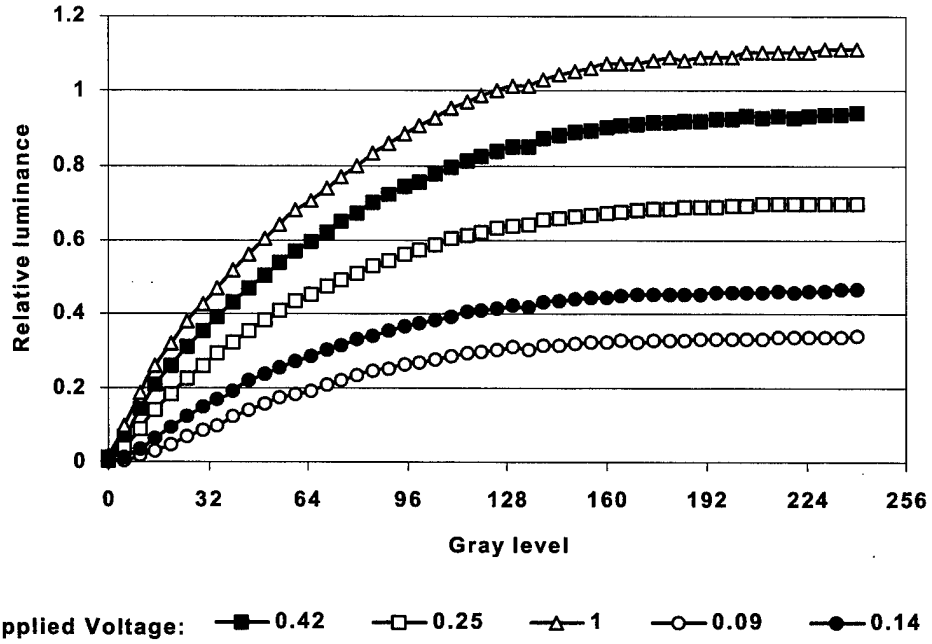

Figure 11. Luminance response curves as a function of applied voltage (expressed in volts).

Discussion: The Gamma curves were orderly in nature and showed a compressive nonlinearity.

L' minance uniformity

Test equipment: CCD video camera with a wide angle lens, monitor, computer, image capture card, and Matrox Image Inspector version 3 software.

Test procedure: The left side display was measured with a driving voltage of 0.1 volt. A 25 square pattern (each square 80 by 60 pixels with a gray level of 255) was presented with the background set to a gray level of 0. The squares were distributed over the viewing area according to the scheme shown below. A 1280 by 960 pixel image was displayed where the center pixels of the squares were positioned at the 10%, 30%, 50%, 70% or 90% position. For example, the center pixel of the top left square was positioned at coordinate (128,96) where the top left corner coincides to coordinate (0,0). The (128,96) position corresponds to the 10% lateral and the 10% down position. The luminance plot in Figure 12 gives the center pixel position in pixels. The display was imaged by a CCD camera with a wide angle lens and captured on computer. The relative luminance was measured using the image software.

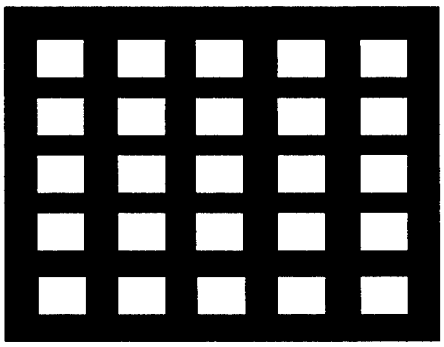

Results: The luminance uniformity results can be seen in Table 3 and are graphically represented in Figure 12. The measurements are given as a percent deviation from the mean luminance. Note that most squares are within ± 20 percent, with the exception of two corner squares.

Table 3.
Luminance uniformity (deviation from the mean).

0.12%	-29.14%	2.69%	-16.82%	5.77%
0.12%	-7.07%	11.42%	1.66%	8.85%
-5.52%	-14.77%	-6.55%	-6.55%	1.15%
6.80%	-8.61%	9.37%	-4.50%	5.77%
8.34%	-0.39%	7.31%	7.31%	23.23%

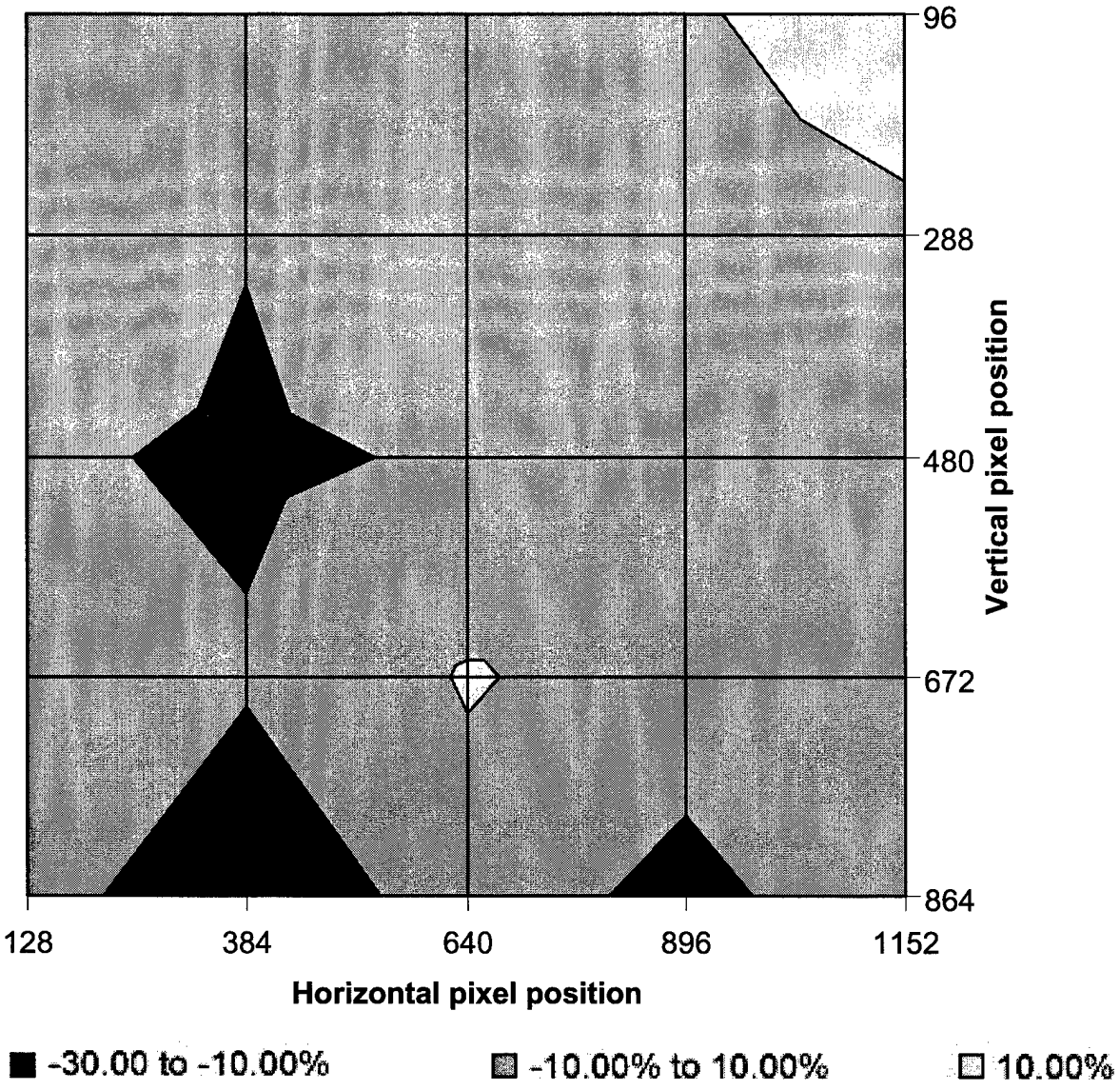

Figure 12. Luminance uniformity of a 25-square pattern dispersed evenly over the entire left side FOV. The display is essentially uniform within ±10% with the exception of five areas.

Discussion: The uniformity was rather good, although 2 of the 25 squares fell outside of the Comanche specification of being within ±20 percent deviation from the mean.

Contrast

Test equipment: CCD video camera with wide-angle lens, monitor, computer, image capture card, and Matrox Image Inspector Software, Version 3.

Test procedure: The left side display was measured with a driving voltage of 0.1 volt. Contrast/contrast uniformity was measured using the same 25 bright square pattern as shown above (Luminance uniformity section). A CCD image of the display was captured by computer and the resulting gray levels measured in the image inspection software. Contrast ratios were measured using two methods. Peak luminance was measured in the middle of each of the 25 squares. Background luminance was measured at points 80 pixels to the left of the center of each square and 80 pixels below the center of each square. Contrast ratios were calculated by dividing the peak luminance by the background luminance to the side of the square (lateral contrast ratios) and beneath the square (vertical contrast ratios).

Results: Tables 4a and b show the contrast ratios for the lateral and vertical contrast, respectively.

Table 4a.
Lateral contrast ratios.

10.05	10.78	11.00	10.45	9.23
10.95	8.48	10.14	9.30	10.30
9.68	8.30	10.11	8.67	10.37
8.13	9.05	10.33	9.90	10.60
9.29	7.26	10.00	8.10	12.12

Table 4b.
Vertical contrast ratios.

10.05	10.21	10.45	9.95	11.43
8.67	8.09	9.68	8.86	9.81
9.20	7.55	8.27	8.67	9.38
9.29	9.05	9.86	9.90	10.60
9.75	6.90	10.53	8.53	10.84

Discussion: The contrast was rather uniform but proved to be somewhat less than measured previously by Rash, et al. (1999). They measured an average lateral contrast of 17.8 and a vertical contrast of 16.7. To be certain of the photographic measurement technique, we confirmed the lower contrast measurements with photometric measurements.

Contrast transfer function (CTF)

Test equipment: CCD video camera with a telephoto lens and 5 mm iris, monitor, computer, image capture card, and Matrox Image Inspector version 3 software.

Test procedure: Grill patterns (vertical and horizontal square wave gratings) of increasing spatial frequency were presented to the left and right sides in order to measure the CTF. The grill pattern was imaged by a CCD camera and captured by computer. The magnification was about 8 pixels in the captured image for each one pixel in the display. This level of magnification allowed measurement of the relative luminance (gray scale) perpendicular to the grill orientation. Spatial frequencies ranged from 20 to 640 cycles per display width in the horizontal meridian (15 to 480 cycles per display in the vertical meridian). These frequencies relate to a grill expression of columns or rows of 32 pixels on, followed by 32 pixels off, and so on, up to 1 pixel on followed by 1 pixel off. These patterns relate to nominal fundamental spatial frequencies of 0.5 cycles per degree (c/deg) to the Nyquist frequency of 16.0 c/deg (these numbers are based on a nominal FOV of 30 by 40 degrees).

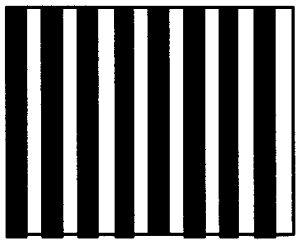

Results: Characteristic CTFs for the left and right side displays are shown in Figures 13a and b, respectively. In all, we measured CTFs for a range of drive voltages and found no appreciable change. Michaelson contrast was calculated from the luminance/gray level data in the captured image. Michaelson contrast is defined as $(L_{max} - L_{min})/(L_{max} + L_{min})$.

Discussion: The CTFs show minor improvement from those measured previously (Rash et al., 1999). At the Nyquist frequency (approximately 16 c/deg), the contrast was about 0.2 for the horizontal grill pattern. This compares favorably to no appreciable modulation found previously for this frequency. The horizontal grill CTF should provide slightly higher contrast modulation at these higher frequencies since the grill is constructed of single scanned lines. Visually observing the highest spatial frequency under magnification, we failed to notice any significant luminance modulation for the vertically oriented grating. Microvision engineers suggest that new electronics will improve contrast at the Nyquist frequency as Comanche specifications calls for modest contrast at this frequency.

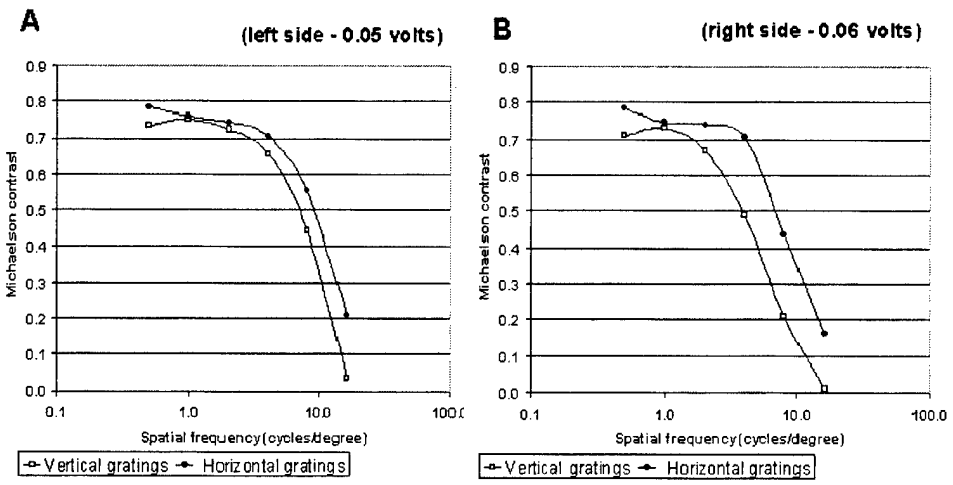

Figure 13. Typical CTFs for the left (A) and right (B) sides. Note the similarity between the two sets of curves. CTFs for horizontal gratings are always higher although the separation between the curves could vary as a function of focus and alignment of the laser beams.

Modulation transfer function (MTF)

Test equipment: CCD video camera with a telephoto lens and 5 mm iris, monitor, computer, image capture card, Matrox Image Inspector Software, Version 3, and Fast Fourier Transform (FFT) software.

Test procedure: A single vertical or horizontal line in the middle of the display was imaged by a CCD camera and the image captured and stored on a computer for analysis. Approximately eight pixels in the captured image equaled one pixel in the display. The line profile or line spread function, from the captured image, was frequency transformed and the MTF calculated. The MTF was normalized to one at zero frequency.

Results: The MTFs for the left side are shown in Figure 14. The difference between the horizontal and vertical MTFs can be positively compared to the CTFs in Figure 13.

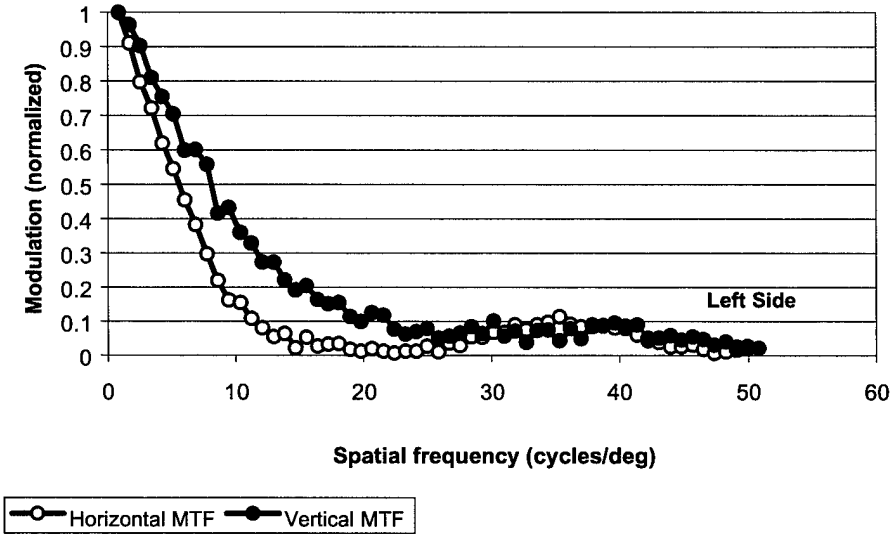

Figure 14. Left side MTFs.

Discussion: The horizontal MTF has a faster roll-off than Comanche program specifications dictate. No appreciable modulation was measured at the 16 c/deg Nyquist frequency for the horizontal MTF. Again, the noted modulation of the vertical MTF at the Nyquist frequency is an improvement over USAARL's earlier evaluation (Rash, et. al., 1999).

Interpupillary distance (IPD) and vertical adjustments

Test equipment: Exit pupil location device consisting of a section of rear screen projection material sandwiched between circular metal clamps, optical assembly with clamps and rod, and a millimeter rule.

Test procedure: Both optical channels were centered. The positions of the left and right exit pupils were found using the rear projection screen. The distance between the two positions was measured. The maximum IPD was measured as a function of the vertical adjustment. To measure the vertical alignment, a marker was placed on the combiner lens assembly, which allowed measurement of the vertical extent with a millimeter rule.

Results: The eyepieces could be moved up and down over a 10 mm range. The IPD scale reads 58 to 74 mm, but the range of motion will not extend out to 74 mm. We measured the IPD range to be 57 to 73 mm.

Discussion: The vertical travel and IPD range appear sufficient.

See-through color discrimination

Test equipment: Dvorine Pseudo-Isochromatic plates, Lanthony's desaturated D-15 hue test, and a MacBeth easel lamp.

Test procedure: Three observers with normal color vision were tested using the Dvorine Pseudo-Isochromatic plates and the Lanthony's desaturated D-15 hue test. The Dvorine test consisted of 14 test plates viewed under a MacBeth easel lamp. The observers viewed plates and read the embedded numbers while wearing the helmet mounted display. No more than 5 seconds were allowed per plate. The Lanthony test consisted of 16 color chips (embedded in circular caps) selected from the Munsell Book of Color, and the chips were viewed under the MacBeth easel lamp. The hues (Munsell hues) were selected so that the intervals between different hues were approximately equal. The mean chroma (Munsell chroma) was 2 and the mean luminosity level (Munsell value) was 8. The color caps had scoring values on the bottoms. A reference cap was fixed permanently to the left end of the lower panel of the rack. The remaining 15 caps were placed in random order on the upper panel of the rack. The observers' task was to arrange the color chip caps in order according to color similarity. They were instructed to do this by first locating the color caps that most closely resembled the reference cap and placing it next to it, and then selecting the color cap that most closely resembled the last selected cap, etc., until all of the caps were arranged in order. By closing the rack and turning it over, the scoring numbers became visible and the observer could be scored.

Results: All observers correctly identified the isochromatic plates, although with some difficulty. Likewise, the D-15 test was completed successfully by all observers. However, it was noted that the first five chips could be successfully ordered yet their appearance clearly lacked a green tint, which made ordering more difficult.

Discussion: As these tests are designed to catch color discrimination deficiencies based upon cone deficiencies, they may not provide the best measurement of color discrimination deficiencies due to the lens coatings in the HMD. Certainly some discriminations will be more difficult, and this leads to increases in reaction time for tasks that require accurate color discrimination.

Problematic issues associated with jitter

During testing, we found possible problems that were not addressed with our testing procedures, and these problems did not lend themselves to immediate evaluation. One of these issues was the jitter that occurs that essentially locates a pixel at multiple locations on sequential frames (rewrites). We are not sure of the best method to characterize jitter since a method of spatially sampling pixel position is not a trivial task and requires high speed spatial sampling. However, one method is to characterize jitter by the diameter of the spatial spread of pixel positions. This method may provide a measure of the extent of the spatial smear but it does not provide the frame-to-frame details of the jitter that could be characterized by a spatiotemporal metric. Further, we are not certain about the visual performance consequences of jitter. We do know that jitter will cause smearing of temporally summed imagery. From a psychophysical point of view, we know that the spatiotemporal surface that describes visual sensitivity shows that high spatial frequencies are detected by low to moderate temporal frequency mechanisms. That is to say that high spatial frequency/high temporal frequency targets are much harder to detect, recognize and identify than high spatial frequency/low temporal frequency targets. That there may be a high spatial frequency deficit would be characterized by a loss of sensitivity to fine details in imagery. It would have little to no effect upon the readability of typical symbology. Its deficits would generally be constrained to video imagery from FLIR or image intensification sources.

We can surmise from the diameter of the jitter spread what frequencies would be directly affected. For example, visual detection of targets whose frequency spectrum contains frequencies that approach the display's Nyquist frequency would be greatly affected by jitter whose spread is greater than the pixel pitch. Much of the jitter or drift that we noticed was due to interference between the left and right channels lap top computers and cables. This jitter exceeded several pixel pitches. With one channel turned off and its cable disconnected, the jitter could be reduced to about a pixel pitch.

Safety issue

During a last recheck on luminance values, the laser scanning mechanism suffered an apparent failure. As a result, the laser image was reduced to a single point within the FOV. This represents an ocular safety hazard. Designed safety interlocks within the system should have shut the laser down by removing power to the laser. This incident was reported to Microvision.

Summary and discussion

Evaluation results are summarized in Table 5. The Microvision laser HMD demonstrated the feasibility of this concept and offered some advantages over more mature technologies. The high luminance output of the system was the single greatest advantage.

The greatest deficiency noted was the rather poor contrast ratios for the 25 square pattern and the MTF and CTF for vertical bars. Luminance uniformity was rather good although several measurements fell outside the ±20 percent Comanche requirement.

Additional areas of concern were the amount of jitter and the poor pixel alignment in columns. Discussions with Microvision engineers indicate the alignment problem will be fixed when new electronics are incorporated into the system.

Other problems noticed were the amount of crosstalk/interference between the cables and the two laptop computers that were used to provide imagery to the two sides of the HMD. Often, one laptop had to be turned off and the cables unplugged in order to eliminate the interference in the channel under evaluation.

The final issue, and one of supreme importance, was the scanning failure which was not accompanied by an appropriate removal of electrical power to the laser. Microvision has in the past outlined a comprehensive plan for addressing safety concerns with this system. However, in view of the noted failure in the "on" mode, it is strongly recommended a formal evaluation of the possible failure modes be required by the Air Crew Helmet Sighting (AIHS) program.

Table 5.
Evaluation summary.

Exit pupil size and shape	Approximately 15 mm and circular
Eye relief	Physical eye relief: 19 mm nominally; Optical eye relief: 42 mm nominally
Field-of-view (FOV)	Slightly greater than 30 by 40 degrees monocularly
Binocular FOV and overlap	Horizontal: 53.24 degrees; Vertical: 31.6 degrees; Overlap 25 degrees
Binocular alignment	Less than one milliradian
Transmissivity	Photopic transmission: 59.3% with a tungsten source
Spectral output	Highly monochromatic with a peak at 534 nm
Aberrations	Field curvature was generally negative but did not exceed -1 diopter. Astigmatic error did not exceed 0.5 diopter
Luminance response (Gamma)	Maximum luminance 1485 fL; Compressive nonlinearity
Luminance uniformity	8% of area showed greater than ±20% deviation from the mean
Contrast	Contrast ratios measured using the 25 pattern was poor and averaged ~10
Contrast transfer function (CTF)	Poor high frequency response for vertically oriented imagery
Modulation transfer function (MTF)	Poor high frequency response for vertically oriented imagery
IPD and vertical adjustments	IPD range: 57 to 73 mm; vertical range: 10mm
See-through color discrimination	Minor degradation due to notch filter of lens coatings

Reference

Rash, C.E., Harding, T.H., Martin, J.S., and Beasley, H.H., 1999. Concept phase evaluation of the Microvision, Inc. aircrew integrated helmet system HGU-56P virtual retinal display. Fort Rucker, AL: U.S. Army Aeromedical Research Laboratory. USAARL Report No. 99-18.

Appendix.

List of manufacturers.

Gentex Corporation
Carbondale, PA 18409

Matrox Electronic Systems
1055 St. Regis
Dorval (Quebec)
Canada H9P 2T4

Melles Griot
2985 Sterling Ct.
Boulder, CO 80301

Microvision, Inc.
19910 North Creek Parkway
P.O. Box 3008
Bothell, WA 98011

Oriel Corporation
250 Long Beach Blvd
P.O. Box 872
Stratford, CT 06497

Photo Research
3000 North Hollywood Way
Burbank, CA 91505

DEPARTMENT OF THE ARMY
U.S. Army Aeromedical Research Laboratory
Fort Rucker, Alabama 36362-0577